2024 IEEE/RSJ International Conference on Intelligent Robots and Systems (IROS)
October 14-18, 2024. Abu Dhabi, UAE

Robotic valve turning: axial misalignment estimation from reaction torques

Gautami Golani, Sri Harsha Turlapati, Lin Yang, Mohammad Zaidi Bin Ariffin and Domenico Campolo*

***Abstract*— In this work, we present a simplified quasi-static model of a two-point contact gripper turning a circular valve to predict the reaction torques produced at the base of the valve as a function of the axis misalignment. Specifically, we learned that *geometric features* such as (i) the misalignment vector being tangent to the reaction torques, (ii) length of the misalignment vector being directly proportional to the magnitude of the reaction torques and (iii) small axial misalignments resulting in well defined 'double-loops' in the 2D reaction torques space are indicative of axis misalignment.**

I. Introduction

Almost on a daily basis, humans deal with tasks such as rotating a doorknob, inserting a key into a keyhole, twisting a bottle cap, or fixing a light bulb. All these tasks involve rotation of the hand about a fixed axis. Humans seem to be effortlessly able to adapt the hand/arm axis of rotation to the fixed axis. When a similar task has to be automated, e.g. a motor is to be connected to a valve or a wheel, a typical (and necessary) solution is to adopt a *flexible coupler*. The reason is that a misalignment, albeit small, is unavoidable and the function of the coupler is to absorb any kinematic inconsistency between the motor and the load.

These problems are also well known in the field of mechanical vibrations, e.g. see [1], where offsets between two shaft centerlines of rotation can cause axis misalignment producing high reaction torques. Also in this case, flexible couplings allow to control the vibrations due to misalignment by selecting the location of coupling [2]. While at high rotational speeds, vibrations and noise represent a primary indicator of misalignment, at low speed, reaction forces and torques, can be used to quantify misalignment [3]. In this work, we shall focus on quasi-static valve turning via a robotic gripper, as depicted in Fig. 1. We shall specifically focus on single-hand valve turning, as opposed to dual arm, whereby a standard robotic gripper is used to i) pre-position itself, ii) firmly grasp the valve, iii) turn to open/close the valve in presence of small but unavoidable misalignments.

Approaches to autonomous valve turning have already been proposed, often based on force control strategies such as that used by Ahmadzadeh et. al [12]. The reaction forces/torques were dissipated by specifying limits and running a hybrid force controller to match demonstration forces. Abu-Dakka et. al [13] proposed a learning from demonstration (LfD) framework to learn force-based variable impedance for various manipulation tasks with different stiffness levels. The authors do not consider reaction forces but make use of forces recorded during demonstration of valve turning. Yoon et al [14] showed how a circular valve can be manipulated through task skill transfer using hybrid impedance/force control. Additionally, angular misalignment between the screw and the mating hole is an important consideration also in automated threaded fastening using robots [7]. Correcting such axial misalignment to avoid damage caused due to excessive force [11], [12] is important and depicted in Fig. 1.

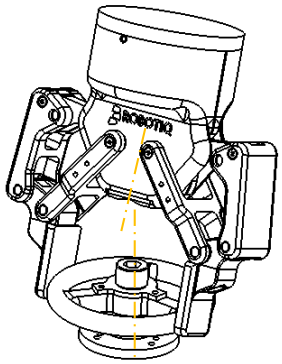

Fig. 1: Valve turning using parallel jaw gripper with axis misalignment.

This work focuses on the *geometric* relationship between reaction torques and axial misalignment. First, by means of a simplified fingerpad-valve compliant interaction, and quasi-static assumptions, we vary axis misalignment methodically and learn that the reaction torques form an ellipse in the torque space. Notably, the misalignment vector is observed to be *tangent* to the torque ellipses. Second, in line with the expectation that a greater axial misalignment would lead to greater reaction torques, we study that the *length* of the misalignment vector is directly proportional to the reaction torque ellipse size. Finally, we also show how small axial misalignments result in well defined 'double-loops' in the 2D reaction torques space (the torque along the axis assumed null following our quasi-static assumptions). In this work, we show how such 'double-loops' also appear during experiments, qualitatively in good agreement with predictions from our simplified model.

The rest of the paper is organized as follows: The proposed quasi-static model is presented in Section II, with details on the expected torque profile and its relation to the misalignment vector. Section III comprises of the experimental validation of the model with the conclusion in Section IV.

All authors are with the Robotics Research Centre, School of Mechanical and Aerospace Engineering, Nanyang Technological University, Singapore
*Corresponding Author: d.campolo@ntu.edu.sg

This research is supported by the National Research Foundation, Singapore, under the NRF Medium Sized Centre scheme (CARTIN).

II. Quasi-static modeling of misalignment

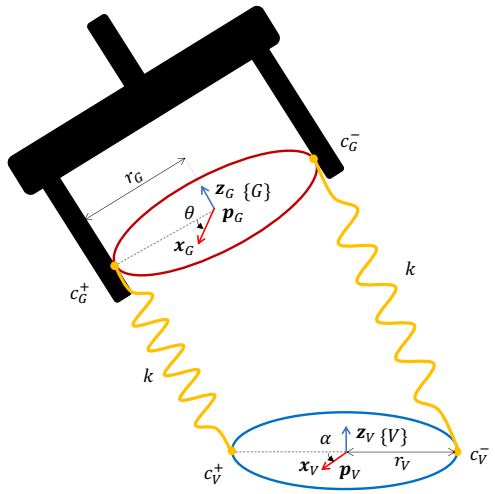

Fig. 2: Elastic interaction between gripper and valve is modeled by stiffness k. The axial misalignment is captured by the relative orientation of $\boldsymbol{z}_G$ and $\boldsymbol{z}_V$.

In this section, we present a quasi-static contact model between a robot's gripper and a circular valve. We assume that the robot gripper is already brought in position and is in contact with the valve. From the valve frame of reference, we assume a small but non-zero misalignment between the z-axis of the valve, along $[0\ 0\ 1]^T \in \mathbb{R}^3$, and the axis of the gripper (coincident with the last joint of the robot), taken parallel the vector $[n_1\ n_2\ 1]^T \in \mathbb{R}^3$, with $(n_1^2 + n_2^2) \ll 1$ denoting the small misalignment. If the robot and the valve were perfectly rigid objects, it would not be possible for the robot gripper to rotate in presence of non-zero misalignment. Similarly to a flexible coupler, the compliance in the robotic fingers / finger-pads absorbs any kinematic inconsistency. Next, we propose to capture this behaviour by assuming a lumped compliance at the point of contact between the fingers and valve. Given this compliance, any kinematic inconsistency will give rise to a strain energy (elastic potential) and, under quasi-static assumptions, its minimum will determine the equilibrium condition, from which elastic reaction torques can be evaluated.

A. Kinematics

With reference to Fig. 2, a gripper with frame $\{G\}$ is misaligned with respect to a valve with frame $\{V\}$.

$$\boldsymbol{x}_V = \begin{bmatrix}1\\0\\0\end{bmatrix}, \quad \boldsymbol{y}_V = \begin{bmatrix}0\\1\\0\end{bmatrix}, \quad \boldsymbol{z}_V = \begin{bmatrix}0\\0\\1\end{bmatrix}, \quad \boldsymbol{p}_V = \begin{bmatrix}0\\0\\0\end{bmatrix}. \tag{1}$$

Denoting the misalignment of the two frames, the vertical axis, $\boldsymbol{z}_G$ is given by:

$$\boldsymbol{z}_G = \frac{1}{\sqrt{n_1^2 + n_2^2 + 1}} \begin{bmatrix}n_1\\n_2\\1\end{bmatrix}, \quad \boldsymbol{p}_G = \begin{bmatrix}d_1\\d_2\\d_3\end{bmatrix}. \tag{2}$$

Consider the plane containing $\boldsymbol{p}_G$ and $\boldsymbol{z}_G$. Under assumptions of small misalignment, i.e. $n_1^2, n_2^2 \ll 1$, the cross product $\boldsymbol{z}_G \times \boldsymbol{x}_V$ is far from being null and the following definition is far from singularity:

$$\boldsymbol{y}_G = \frac{\boldsymbol{z}_G \times \boldsymbol{x}_V}{\|\boldsymbol{z}_G \times \boldsymbol{x}_V\|}, \quad \boldsymbol{x}_G := \boldsymbol{y}_G \times \boldsymbol{z}_G. \tag{3}$$

Note that, by definition, $\boldsymbol{x}_G$, $\boldsymbol{y}_G$ and $\boldsymbol{z}_G$ form an orthonormal system. The contact points on the gripper are parameterised by θ:

$$\boldsymbol{c}_G^+(\theta) = r_G(\cos(\theta)\boldsymbol{x}_G + \sin(\theta)\boldsymbol{y}_G) + \boldsymbol{p}_G, \tag{4}$$
$$\boldsymbol{c}_G^-(\theta) = c_G^+(\theta + \pi). \tag{5}$$

Similarly the valve contact points are parameterised by α as:

$$\boldsymbol{c}_V^+(\alpha) = r_V(\cos(\alpha)\boldsymbol{x}_V + \sin(\alpha)\boldsymbol{y}_V) + \boldsymbol{p}_V, \tag{6}$$
$$\boldsymbol{c}_V^-(\alpha) = c_V^+(\alpha + \pi). \tag{7}$$

B. Strain Energy

We shall model the interaction between gripper and valve simply via elastic deformation of linear springs with stiffness k between the pairs of points $(\boldsymbol{c}_G^+, \boldsymbol{c}_V^+)$ and $(\boldsymbol{c}_G^-, \boldsymbol{c}_V^-)$. The elastic potential energy $E(\alpha, \theta)$ can be written as:

$$E(\alpha, \theta) = \frac{1}{2}k\|\boldsymbol{c}_G^+(\theta) - \boldsymbol{c}_V^+(\alpha)\|^2 + \frac{1}{2}k\|\boldsymbol{c}_G^-(\theta) - \boldsymbol{c}_V^-(\alpha)\|^2$$

Since turning the gripper means actuating θ, the gradient of the contact potential may be interpreted as the torque acting on the gripper $\tau_G = \nabla_\theta E$. For a freely rotating valve (i.e., without friction or inertial effects), the quasi-static contact condition means:

$$\nabla_\theta E = 0 \tag{8}$$

The kinematics of the contact parameter can be deduced by solving this equilibrium equation $\nabla_\theta E = 0$ for θ^*:

$$\theta^*(\alpha) = \arctan 2(-n_1 n_2 + \sqrt{n_1^2 + n_2^2 + 1}\tan(\alpha), n_2^2 + 1)$$

C. Torque expectation for misalignment

The force acting on the valve $\boldsymbol{f}_V$ should be equal and opposite to the reaction on the gripper $\boldsymbol{f}_G$ and will be the sum of forces acting at the two contact points, i.e., $\boldsymbol{f}^+$ at $\boldsymbol{c}_V^+$ and $\boldsymbol{f}^-$ at $\boldsymbol{c}_V^-$ as:

$$\boldsymbol{f}^+ = k(\boldsymbol{c}_V^+(\alpha) - \boldsymbol{c}_G^+(\theta)), \tag{9}$$
$$\boldsymbol{f}^- = k(\boldsymbol{c}_V^-(\alpha) - \boldsymbol{c}_G^-(\theta)), \tag{10}$$
$$\boldsymbol{f}_V(\alpha, \theta) = \boldsymbol{f}^+ + \boldsymbol{f}^-. \tag{11}$$

Therefore, the torque acting on the valve $\boldsymbol{\tau}_V$ will be due to the cross product of the moment arm of the contact points and the force acting at those locations:

$$\boldsymbol{\tau}_V(\alpha, \theta, n_1, n_2) = \boldsymbol{c}_V^+ \times \boldsymbol{f}^+ + \boldsymbol{c}_V^- \times \boldsymbol{f}^-$$

Note that $\boldsymbol{\tau}_V = [\tau_x\ \tau_y\ \tau_z]^T \in \mathbb{R}^3$ and in the following analysis (see Fig. 3) we fix $k = 10000Nm^{-1}$, $r_G = 45mm$, $r_V \approx 43mm$ and $\boldsymbol{p}_G = [5mm\ 5mm\ 5mm]^T$ to plot $\boldsymbol{\tau}_V(\alpha, \theta^*(\alpha), n_1, n_2)$ for *half-rotation* $\alpha \in [-\frac{\pi}{2}\ \frac{\pi}{2}]$.

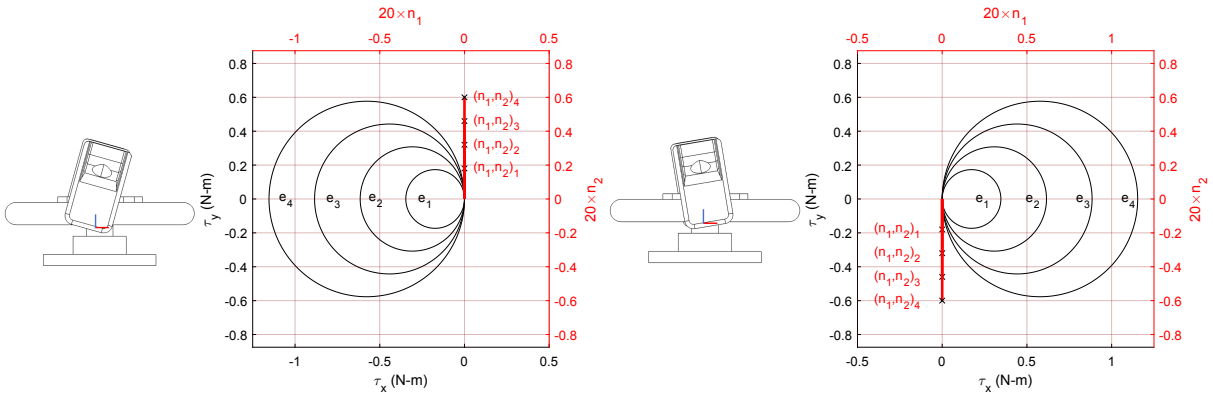

(a) Variation n_2^+ (b) Variation n_2^-

Fig. 3: In this work we present variations along n_2 - increment is denoted by n_2^+ and decrement by n_2^- resulting in expected torque space ellipses along x-axis with $n_1 = 0$. Note that for every i-th variation $(n_1, n_2)_i$ the corresponding torque ellipse e_i is labeled.

The interaction force between two bodies occurs as a result of surface deformation at the contact point/patch. Typically, this deformation can be quantified by the penetration depth along the surface normal of the softer body. In this work, we simplify this notion by defining a force acting on the contact point of the valve from the gripper by connecting a linear spring between them. Specifically, the spring models the stiffness of the foam patch attached to the gripper teeth which deforms upon contact. Once contact occurs, a compression of the spring is modelled by the product of the stiffness and the penetration depth.

We characterise the numerical results of reaction torques during quasi-static valve turning with three key observations:

- A single *torque space* ellipse e is produced for a *half rotation* of the valve, i.e., $\alpha \in [-\frac{\pi}{2}\ \frac{\pi}{2}]$.
- The length of the vector (n_1, n_2) is proportional to the size of the torque ellipse.
- The vector (n_1, n_2) is always tangent to the torque ellipse.

Finally, we expect for a full rotation of the valve to produce two ellipses. We validate these predictions through experimental results in section III.

TABLE I: Nomenclature for the model

Variables	Symbols
Frame associated with the gripper	$\{G\}$
Frame associated with the valve	$\{V\}$
Gripper contact parameter (controlled variable)	θ
Valve contact parameter (uncontrolled variable)	α
Radius w.r.t gripper	r_G
Radius w.r.t valve	r_V
Misalignment errors	n_1, n_2
Grasping points on the gripper	c_G^+, c_G^-
Grasping points on the valve	c_V^+, c_V^-
Stiffness of surface material on the gripper	k
Energy potential	E
Forces	$\boldsymbol{f}_G, \boldsymbol{f}_V$
Torques	$\boldsymbol{\tau}_G, \boldsymbol{\tau}_V$

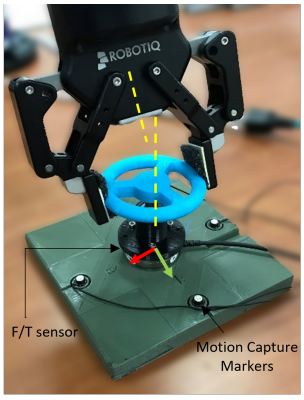

Fig. 4: Experimental setup with a F/T sensor to capture data during rotation and motion capture markers for estimating the position of the valve with respect to the robot.

III. Experimental Validation

In this section, the experimental setup for robotic valve turning equipped with a ATI Mini40 force/torque (F/T) sensor is detailed. The sensor was positioned beneath the valve to measure the torques applied during valve rotation, as seen in Fig 4. Before performing the experiment, it is important to calibrate both the robot arm and the F/T sensor being used to carry out the experiment, described in the Appendix IV. The experimental setup for the valve turning task comprised of a Kinova Gen3 robot arm with $D = 7$ degrees of freedom, equipped with torque sensors at each joint allowing for gravity compensation and thus human robot interaction, to allow for manual guiding of the robot into the valve turning posture. The valve was designed with a bearing inserted between the rotor and housing for smooth rotation of the valve with no friction. It must also be ensured that the valve prototype consists of little to no wobbling.

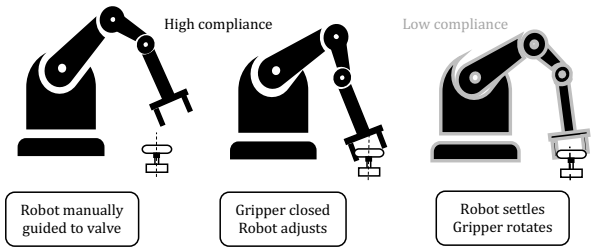

Fig. 5: High compliance mode allows robot to *adjust* to reaction forces/torques.

A. Protocol

The experiment was carried out to accommodate 2 variations by rotating the robot gripper about the horizontal axis, i.e., by varying n_2. The gripper was then closed and the proximal joints of the robot were allowed to *adjust* to a mechanical equilibrium minimizing the reaction torques originating at the end-effector by using a *high compliance* control mode (see Fig. 5). Once the robot *settled* at the equilibrium, the proximal joints were stiffened up to a *low compliance* mode with a high stiffness ($K_d = 0.5\frac{Nm}{deg}\ \forall d \in [1 \dots D]^T$) to avoid any changes to the set misalignment. The gripper joint was then actuated to multiple rotations under torque control. As the valve is turned, the reaction torques at the base are recorded. Finally, in the end the gripper is disengaged from the valve safely.

B. Analysis of valve torques

First we present the results of multiple rotations of the valve and observe the tangency of (n_1, n_2) to the *torque space* ellipses in Fig. 6. The gripper was turned continuously with each full turn taking about $10sec$ as seen in Fig. 7b.

Since experimental data consists of multiple observations of $\boldsymbol{z}_G(t)$, we first express these in terms of $\tilde{n}_1(t)$ and $\tilde{n}_2(t)$. Next we *estimate* the gripper axis misalignment as an average $(\hat{n}_1, \hat{n}_2)$ computed over the entire duration of rotation when the gripper was in contact with the valve. Specifically, we have the *re-calibrated* robot feedback data $\boldsymbol{z}_G = [z_{G,x}\ z_{G,y}\ z_{G,z}]^T$ which indicates the axis of gripper satisfying the following similarity condition:

$$\frac{\tilde{n}_1}{\tilde{n}_2} = \frac{z_{G,x}}{z_{G,y}} \tag{12}$$

Furthermore, the unitary condition is satisfied as:

$$\sqrt{z_{G,x}^2 + z_{G,y}^2 + z_{G,z}^2} = 1 \tag{13}$$

We utilise the ratio (eq. 12) as:

$$\tilde{n}_1(t) = \text{sgn}(z_{G,z}(t))\frac{z_{G,x}(t)}{z_{G,z}(t)}, \tag{14}$$

$$\tilde{n}_2(t) = \text{sgn}(z_{G,z}(t))\frac{z_{G,y}(t)}{z_{G,z}(t)}. \tag{15}$$

where $\text{sgn}(\cdot)$ evaluates the sign of the argument. Once the gripper axis in terms of $\tilde{n}_1(t)$ and $\tilde{n}_2(t)$ is obtained using experimental data for each time instance, an average $(\hat{n}_1, \hat{n}_2)$ is computed and used to denote the gripper axis misalignment in the torque space plots which are plotted on top of the *torque space* ellipses for each variation as seen in Fig. 6. As expected this vector was tangent to the torque space ellipses.

1) Frequency of reaction torques in single-turn analysis: Beyond the tangency of $(\hat{n}_1, \hat{n}_2)$ to the torque ellipses, we also study the frequency of reaction torques compared to the frequency of rotation. Specifically, it was discussed in section II-C that for every full-turn of the valve, a *double loop* is produced in the torque space. Such double loops are in agreement with the double frequency reported in mechanical vibration literature. Specifically, it was reported in [4], [5] that the frequencies of forces and moments (and therefore vibrations) are *even multiples* of the operating speed of the motor, i.e., frequency of rotation. This is to be expected since, every period of rotation generates also periodically the reaction forces at the uneven loading points. To this end, in our work we plot the gripper parameter with initial condition θ_0 from experimental data and highlight the key checkpoints when $\theta = [0,\ \pi/4,\ \pi/2,\ 3\pi/4,\ \pi] + \theta_0$. We note that, consistent to our expectation in both variations n_2^+ and n_2^-, the frequency of reaction torques was twice the frequency of rotation, i.e., for every one full rotation of the valve, two reaction torque ellipses were traced out as seen in Fig. 7a and Fig. 7b.

In our work, we present a quasi-static misalignment model to compute torques only due to misalignment contact, as long as the contact points don't slip. While greater speeds will bring in dynamics (inertia and Coriolis) of the robot and the valve into consideration, the reaction torques presented in this work will still be a constituent part of those measurements. More importantly, we believe that these will be additive. Further, regardless of the shape of the valve, i.e. circular or elliptical, the key factor for determining the reaction torque ellipses are the two opposite contact points. Since in this work, we assume these contact points do not slip, the reaction torque ellipses will not change once contact has been established with the valve.

IV. Conclusion and Future Scope

In this work, we present a quasi-static model to predict reaction torques as a function of axis misalignment during robotic valve turning task. The physical interaction between the robot gripper and the valve is described as elastic deformation of springs between the two contact points. The interaction potential is computed and we solve for the equilibrium state to compute the equation of motion for the contact parameter and the reaction torques.

We learn that there is a *geometric* relation between the reaction torques and axis misalignment. Specifically, the misalignment vector is *tangent* to the reaction torques and its *length* is proportional to the magnitude of the reaction torques, i.e., greater the misalignment, the greater is the reaction torque. Finally, we also observe that the frequency of torques is twice the frequency of valve rotation, i.e., the

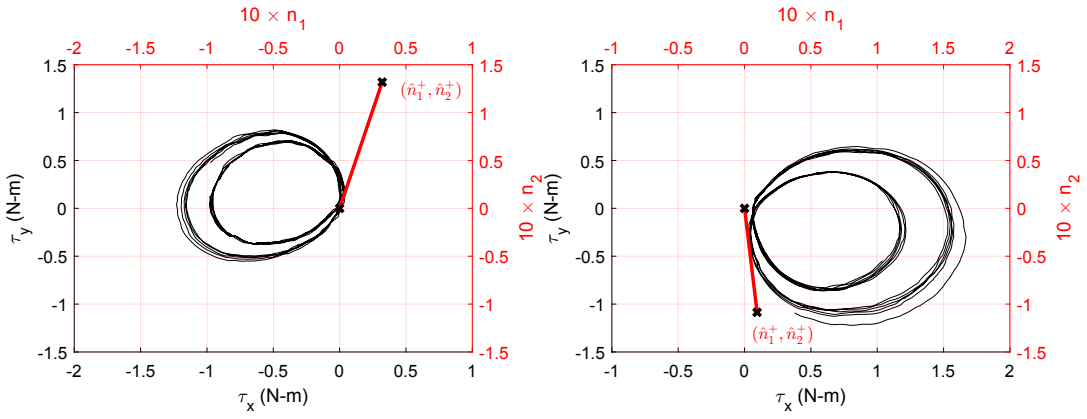

(a) Variation n_2^+ (b) Variation n_2^-

Fig. 6: Resultant τ_x-τ_y plots obtained from the experiments with $(\hat{n}_1, \hat{n}_2)$ tangent to the torque-ellipses.

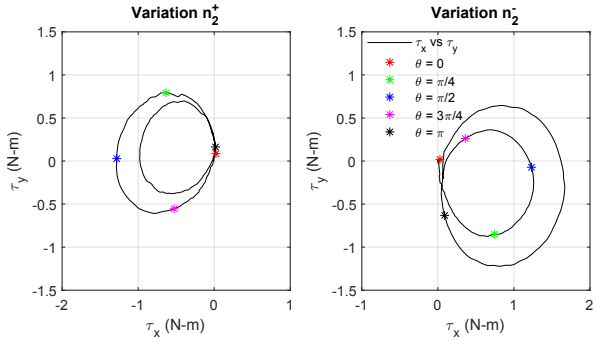

(a) Reaction torque plots for one full rotation

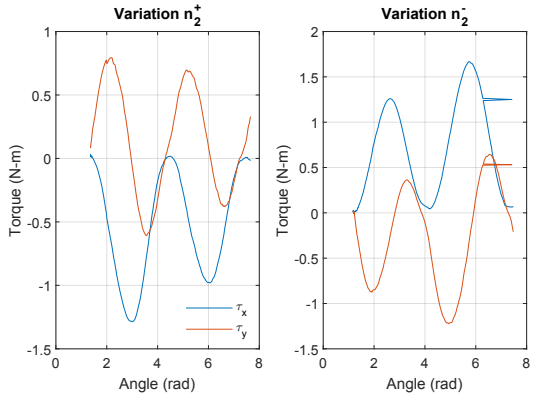

(b) Torque vs gripper contact parameter θ

Fig. 7: Frequency of reaction torque was double the frequency of rotation, i.e., two torque-ellipses per turn.

presence of 'double loops' in the torque-space for every valve rotation.

Additionally, it may not be ideal to expect that the force/torque (F/T) sensor is always co-located with the contact location. For this reason, it would be desirable to use the robot joint torque feedback in such cases to estimate the reaction torques and consequently the robot's axial misalignment with the valve and identify this as a gap. We shall also try to use the tangency condition to reduce the misalignment in future work.

APPENDIX

A. Re-calibration of Robotic Arm

We kinematically re-calibrate the 7DoF Kinova Gen3 robot to accurately estimate gripper orientation, i.e., n_1 and n_2. The forward kinematics of this manipulator can be written as:

$$\boldsymbol{FK}(\boldsymbol{q}) = \boldsymbol{T}_1^B(\boldsymbol{q}_1)\boldsymbol{T}_2^1(\boldsymbol{q}_1)...\boldsymbol{T}_E^D(\boldsymbol{q}_d) = \begin{bmatrix} \boldsymbol{R}(\boldsymbol{q}) & \boldsymbol{p}(\boldsymbol{q}) \\ \boldsymbol{0} & 1 \end{bmatrix} \tag{16}$$

where $\boldsymbol{q} \in \mathbb{R}^D$, D is the number of joints of the robot and $\boldsymbol{T}_d^{d-1}$ is the transformation between the individual joints while $\{B\}$ and $\{E\}$ denote the frame of the robot base and end-effector. The orientation and position of the end-effector are represented by $\boldsymbol{R}(\boldsymbol{q}) \in SO(3)$ and $\boldsymbol{p}(\boldsymbol{q}) \in \mathbb{R}^3$, respectively. Although this is the kinematic model, the true robot kinematics must always be estimated through experiments to overcome the calibration issues caused due to manufacturing and assembly process of the robot. We denote the re-calibrated kinematic model as:

$$\widetilde{FK}_{l+\boldsymbol{\delta l}}(\boldsymbol{q}+\boldsymbol{\delta q}) = \begin{bmatrix} \boldsymbol{R}(\boldsymbol{q}+\boldsymbol{\delta q}) & \boldsymbol{p}_{l+\boldsymbol{\delta l}}(\boldsymbol{q}+\boldsymbol{\delta q}) \\ \boldsymbol{0} & 1 \end{bmatrix} \tag{17}$$

where, we use the fast kinematic re-calibration model devised in [9] to calibrate joint offsets ($\boldsymbol{\delta q} = [\delta q_1, ..., \delta q_D]$) and link length offsets ($\boldsymbol{\delta l} = [\delta l_1, ..., \delta l_{D+1}]$).

To obtain the re-calibrated model, i.e., $\boldsymbol{\delta q}$ and $\boldsymbol{\delta l}$, the robot was commanded with variations in rotation $\boldsymbol{R}$ and position $\boldsymbol{p}$ which were recorded along with the corresponding joint readings $\boldsymbol{q}$. The results are listed in Table II.

B. Force/Torque Sensor Calibration

It is important to calibrate the ATI Mini40 sensor to detect and measure precise and reliable force/torque values. For this, we have used the methodology presented in [10], where two important parameters related to the sensor's performance

TABLE II: Robot re-calibration results

Frame	$\boldsymbol{\delta q}$ (rad)	$\boldsymbol{\delta l}$ (m)
Base	NA	NA
Frame 1	0.0081	[0.0009, 0.0015, 0.0008]
Frame 2	0.0006	[-0.0007, -0.0029, 0]
Frame 3	-0.0013	[0.0013, 0, 0]
Frame 4	0.0060	[0.0011, -0.0000,-0.0016]
Frame 5	-0.0058	[-0.0001, 0.0001, 0]
Frame 6	-0.0008	[-0.0005, -0.0037, 0]
Frame 7	0.0123	[-0.0004, 0.0003, 0]
End-effector	NA	[0.0023, 0.0005, 0]

were modeled, namely the bias and the gain. F/T sensors have biases (offsets), meaning that the sensor will measure non-zero readings even though there is no movement and no external load acting on the sensor. This maybe caused due to manufacturing errors, environmental factors or long term wear and tear. Gain, on the other hand, refers to the change in the sensor's input given a change in force or torque.A static range (no load) was identified from the dataset and measured forces were compared with the expected ones. For each force measurement, f_i,

$$\left(\frac{f_{xi}-f_{0x}}{c_x}\right)^2+\left(\frac{f_{yi}-f_{0y}}{c_y}\right)^2+\left(\frac{f_{zi}-f_{0z}}{c_z}\right)^2=\|f_i\|$$

where, $\boldsymbol{f}_0^T$ is the bias and $\boldsymbol{c}=[c_x,c_y,c_z]^T$ is the gain. The re-calibrated forces are then computed as:

$$\boldsymbol{f}_{CAL}=diag^{-1}(\boldsymbol{c}).(\boldsymbol{f}_i-\boldsymbol{f}_0) \tag{18}$$

Similarly, for each torque measurement,

$$\boldsymbol{\tau}_{CAL}=\boldsymbol{\tau}_0+diag(g)\boldsymbol{\tau}_i \tag{19}$$

With these, we obtain the wrench as:

$$\boldsymbol{W}_{CAL}=\begin{bmatrix}\boldsymbol{f}_{CAL}\\ \boldsymbol{\tau}_{CAL}\end{bmatrix} \tag{20}$$

ACKNOWLEDGMENT

This research is supported by the National Research Foundation, Singapore, under the NRF Medium Sized Centre scheme (CARTIN). Any opinions, findings, and conclusions or recommendations expressed in this material are those of the authors and do not reflect the views of National Research Foundation, Singapore.

REFERENCES

[1] Singiresu, S. Rao. Mechanical vibrations. Boston, MA: Addison Wesley, 1995.

[2] Sekhar, AS A., and B. S. Prabhu. "Effects of coupling misalignment on vibrations of rotating machinery." Journal of Sound and vibration 185, no. 4 (1995): 655-671.

[3] Reddy, M. Chandra Sekhar, and A. S. Sekhar. "Detection and monitoring of coupling misalignment in rotors using torque measurements." Measurement 61 (2015): 111-122.

[4] Xu, M., and R. D. Marangoni. "Vibration analysis of a motor-flexible coupling-rotor system subject to misalignment and unbalance, part I: theoretical model and analysis." Journal of sound and vibration 176, no. 5 (1994): 663-679.

[5] Xu, M., and R. D. Marangoni. "Vibration analysis of a motor-flexible coupling-rotor system subject to misalignment and unbalance, part II: experimental validation." Journal of sound and vibration 176, no. 5 (1994): 681-691.

[6] Bahaloo, Hassan, Alireza Ebrahimi, and Mostafa Samadi. "Misalignment modeling in rotating systems." In Turbo Expo: Power for Land, Sea, and Air, vol. 48876, pp. 973-979. 2009.

[7] Jia, Zhenzhong, Ankit Bhatia, Reuben M. Aronson, David Bourne, and Matthew T. Mason. "A survey of automated threaded fastening." IEEE Transactions on Automation Science and Engineering 16, no. 1 (2018): 298-310.

[8] Mason, Matthew T. "Toward robotic manipulation." Annual Review of Control, Robotics, and Autonomous Systems 1 (2018): 1-28.

[9] Kana, Sreekanth, Juhi Gurnani, Vishal Ramanathan, Sri Harsha Turlapati, Mohammad Zaidi Ariffin, and Domenico Campolo. 2022. "Fast Kinematic Re-Calibration for Industrial Robot Arms" Sensors 22, no. 6: 2295. https://doi.org/10.3390/s22062295

[10] Turlapati, Sri Harsha, and Domenico Campolo. 2023. "Towards Haptic-Based Dual-Arm Manipulation" Sensors 23, no. 1: 376. https://doi.org/10.3390/s23010376

[11] Carrera, A., S. R. Ahmadzadeh, A. Ajoudani, P. Kormushev, M. Carreras, and D. G. Caldwell. "Towards autonomous robotic valve turning." Cybernetics and Information Technologies 12, no. 3 (2012): 17-26.

[12] Ahmadzadeh, Seyed Reza, Petar Kormushev, Rodrigo S. Jamisola, and Darwin G. Caldwell. "Learning reactive robot behavior for autonomous valve turning." In 2014 IEEE-RAS International Conference on Humanoid Robots, pp. 366-373. IEEE, 2014.

[13] Abu-Dakka, Fares J., Leonel Rozo, and Darwin G. Caldwell. "Force-based variable impedance learning for robotic manipulation." Robotics and Autonomous Systems 109 (2018): 156-167.

[14] Yoon, W-K., Takashi Suehiro, Hiromu Onda, and Kosei Kitagaki. "Task skill transfer of circle handle valve manipulation." In ROMAN 2005. IEEE International Workshop on Robot and Human Interactive Communication, 2005., pp. 505-511. IEEE, 2005.